

## Local fields and conduction-electron behavior at impurity sites in indium-doped ZnO

W. Sato,<sup>1</sup> Y. Itsuki,<sup>1</sup> S. Morimoto,<sup>2,3</sup> H. Susuki,<sup>2</sup> S. Nasu,<sup>2</sup> A. Shinohara,<sup>1</sup> and Y. Ohkubo<sup>4</sup><sup>1</sup>Graduate School of Science, Osaka University, Toyonaka, Osaka 560-0043, Japan<sup>2</sup>Graduate School of Engineering Science, Osaka University, Toyonaka, Osaka 560-8531, Japan<sup>3</sup>Faculty of Pharmacy, Osaka Ohtani University, Tondabayashi, Osaka 584-8540, Japan<sup>4</sup>Research Reactor Institute, Kyoto University, Kumatori, Osaka 590-0494, Japan

(Received 25 January 2008; revised manuscript received 16 May 2008; published 22 July 2008)

Local fields in the vicinity of  $^{111}\text{Cd}(\leftarrow^{111}\text{In})$  probes in different ZnO samples—0.5 at.% indium-doped and undoped—were measured by means of the time differential perturbed angular correlation method. Prominent aftereffect observed for the 0.5 at.% In-doped ZnO evidently exhibits an anomalous behavior of conduction electrons at a local scale: the probe site is off the mainstream of carrier electrons despite enhanced electric conductivity in the bulk. A remarkable observation of a drastic and discrete change in the electric field gradient at the probe in the different samples is also presented.

DOI: 10.1103/PhysRevB.78.045319

PACS number(s): 76.80.+y, 61.72.uj, 72.80.Ey

## I. INTRODUCTION

Zinc oxide (ZnO) is one of the most promising compounds in wide fields of technology and industry because of its semiconducting properties applicable to functional devices. It is known that those intriguing physical properties depend on the type and concentration of impurity ions forming shallow donor levels below the conduction band. Since it is extremely difficult to identify the levels due to other co-existing defects in the matrix, however, even the origin of the *n*-type conductivity, for example, is still in controversy.<sup>1-3</sup> This problem is partly originated from the difficulty in clarifying the physical properties associated with impurities by macroscopic observations. In order to understand the functions of impurities in ZnO, accordingly, it is necessary to directly observe what is happening at the impurity sites. If it is possible to make use of impurities as the probe of a spectroscopy, they can provide direct information on the electronic state of themselves. In that sense, nuclear techniques with radioactive probes are very suited for this purpose because of their high sensitivity.

For group II–VI compound semiconductors including ZnO, group III elements are regarded as ideal donors owing to their valence.<sup>4-6</sup> Directing our interest to this group, we doped indium (In) as an impurity element in ZnO and we measured the local field in the vicinity of the dopants by means of the time differential perturbed angular correlation (TDPAC) method with the probe  $^{111}\text{Cd}$  formed in the disintegration of  $^{111}\text{In}$ . The TDPAC method is a nuclear spectroscopic technique, which provides atomic level information on a local scale in matter through hyperfine interactions between probe nuclei and the surrounding spins and charge distribution.<sup>7,8</sup> This advantage is hence expected to give direct information on the extranuclear field of the  $^{111}\text{In}(\rightarrow^{111}\text{Cd})$  probe.

In the course of the microscopic investigation, we have obtained TDPAC spectra showing an intriguing behavior of conduction electrons at In sites in 0.5 at.% In-doped ZnO along with a drastic difference in the electric field gradient (EFG) values at the probe nuclei between the In-doped and undoped ZnO. Showing a temperature dependence of the

damping trend of the well defined TDPAC spectra for the 0.5 at.% In-doped ZnO, we report the microscopic observation unexpected from the result of bulk experiments on electric conductivity: that is, conduction electrons avoid getting access to the probe ions despite their enhanced conductivity.

## II. EXPERIMENT

For the synthesis of 0.5 at.% In-doped ZnO, stoichiometric amount of  $\text{In}(\text{NO}_3)_3 \cdot 3\text{H}_2\text{O}$  of a purity of 99.99% was dissolved in ethanol, and then 99.999% ZnO powder was added in the solution. The suspension was stirred while heated on a magnetic stirrer to evaporate the ethanol until dryness. The uniformly mixed powder and undoped ZnO powder were then separately pressed into disks. They were sintered on platinum plates in air at 1273 K for 3 h. (The purpose of sintering the undoped ZnO was to obtain data under the same experimental condition as for the In-doped sample.) Powder x-ray diffraction patterns are shown in Fig. 1 for the undoped and In-doped samples. It was confirmed that the lattice constants remained unchanged after the doping of 0.5 at.% In and new phases possibly arising from the dopants were not at all detected within the present detection precision. Commercially available  $^{111}\text{In}$  HCl solution was added in droplets onto each of the sintered disks. After the disks were dried up by heat, they again underwent heat treatment in air at 1373 K for 2 h. TDPAC measurements were performed for the undoped and 0.5 at.% In-doped samples at various temperatures for the probe  $^{111}\text{Cd}(\leftarrow^{111}\text{In})$  on the 171–245 keV cascade  $\gamma$  rays with the intermediate state of  $I^\pi=5/2^+$  having a half-life of 85.0 ns.<sup>9</sup> [Note that the term “undoped” denotes here the sample that was not doped with nonradioactive In in the form of  $\text{In}(\text{NO}_3)_3 \cdot 3\text{H}_2\text{O}$ . Radioactive  $^{111}\text{In}$  was doped in both samples.] In the present work, we observed the directional anisotropy as a function of the time interval of the cascade  $\gamma$ -ray emissions by the following simple arithmetic operation:

$$A_{22}G_{22}(t) = \frac{2[N(\pi, t) - N(\pi/2, t)]}{N(\pi, t) + 2N(\pi/2, t)}, \quad (1)$$

where  $A_{22}$  denotes the angular correlation coefficient representing the magnitude of the directional anisotropy of the

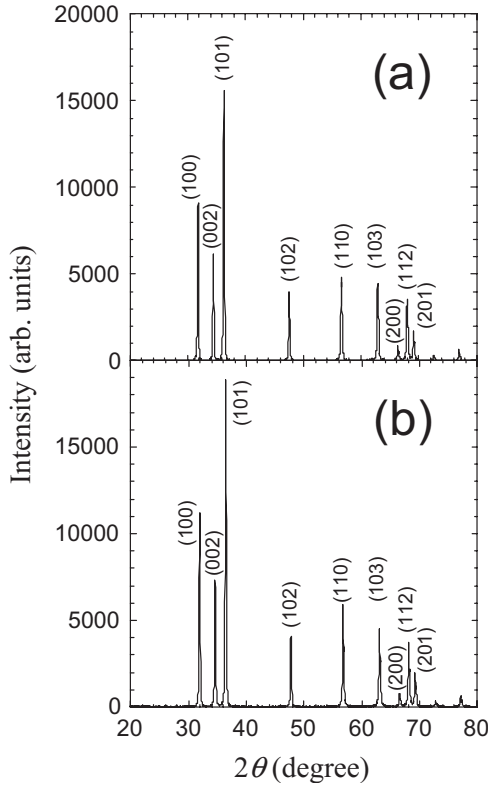


FIG. 1. Powder x-ray diffraction patterns (a) of undoped and (b) of 0.5 at.% In-doped ZnO.

cascade  $\gamma$  rays,  $G_{22}(t)$  the time differential perturbation factor as a function of the time interval,  $t$ , between the cascade  $\gamma$ -ray emissions, and  $N(\theta, t)$  the number of the coincidence events observed at an angle,  $\theta$ . For the  $\gamma$ -ray detection, BaF<sub>2</sub> scintillation detectors were adopted due to their excellent time resolution.

### III. RESULTS AND DATA ANALYSIS

Figure 2 shows the TDPAC spectra of  $^{111}\text{Cd}(\leftarrow^{111}\text{In})$  introduced in the undoped and 0.5 at.% In-doped ZnO measured at various temperatures. Both samples exhibit oscillating patterns typical of electric quadrupole interactions between the probe nucleus and the extranuclear field for the case of the nuclear spin of  $I=5/2$ . From the spectral patterns, one can see two unequivocal facts: (i) there is a large difference of more than three times in the magnitude of the quadrupole frequency between the two samples and (ii) little, if any, temperature dependence is seen in the spectra for the undoped ZnO, whereas for the 0.5 at.% In-doped ZnO the amplitude of the perturbation function is damped and considerably small at room temperature, but it increases with rising temperature.

For the present  $^{111}\text{Cd}(\leftarrow^{111}\text{In})$  probe, there are four different candidates conceivable as the cause of the spectral damping observed for the In-doped ZnO: (i) dynamic perturbations by diffusion of atoms/ions, (ii) distribution of electric quadrupole frequencies arising from different static interactions, (iii) temperature-dependent displacement of the probe

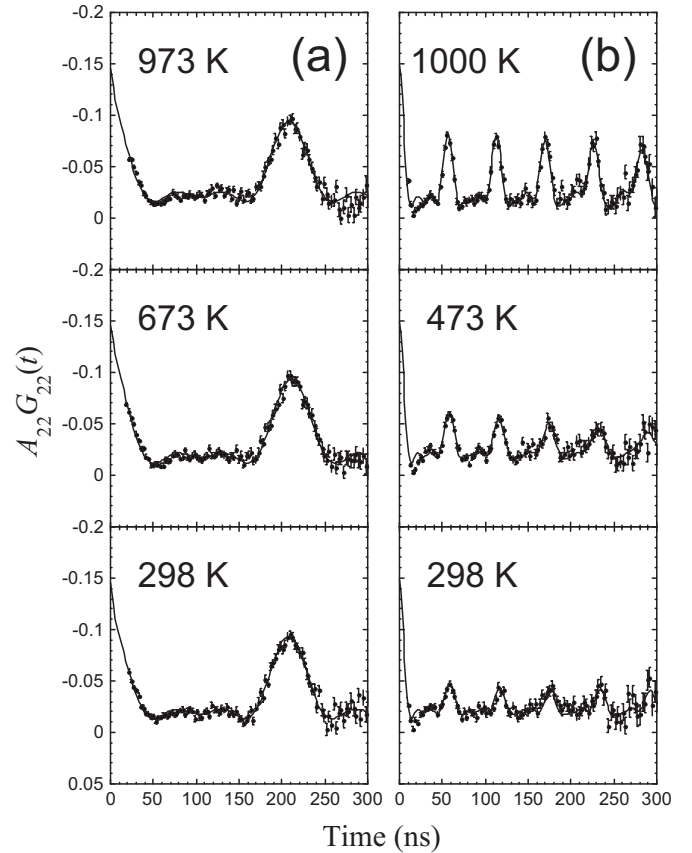


FIG. 2. TDPAC spectra of  $^{111}\text{Cd}(\leftarrow^{111}\text{In})$  embedded (a) in undoped and (b) in 0.5 at.% In-doped ZnO measured at the temperatures indicated.

atoms from site to site, and (iv) the so-called “aftereffect” that takes place in the process of the rearrangement of the orbital electrons of  $^{111}\text{Cd}$  after the disintegration of  $^{111}\text{In}$  via the orbital electron capture.<sup>10,11</sup> For the cases of (i) and (ii), oscillating patterns of a TDPAC spectrum are gradually damped with elapsing time of observation. However, this is not the case with the present results for the 0.5 at.% In-doped sample: the amplitude of the oscillation is retained constantly for the observed time range of 300 ns at any temperature. In addition, we found that the amplitudes of the spectra are reversibly reproduced with respect to the order of the measurements at different temperatures, which excludes the above candidate (iii). The origin of the spectral damping is therefore attributed to the aftereffect. This phenomenon has been observed for this probe especially when embedded in insulators, in which recovery to the ground state of the electronic configuration takes considerably a long time ( $\gg 10^{-8}$  s) due to lack of the conduction electrons.<sup>7</sup> We thus performed the data analysis using the theoretical functions for  $G_{22}(t)$  developed on the aftereffect by Baverstam *et al.*:<sup>12</sup>

$$G_{22}(t) = G_{22}^*(t)G_{22}^{\text{static}}(t). \quad (2)$$

Here,  $G_{22}^*(t)$  is the time-dependent dynamic perturbation part for the damping effect on the static perturbation,  $G_{22}^{\text{static}}(t)$ . The  $G_{22}^*(t)$  is expressed as

TABLE I. Parameter values obtained by least-squares fits on the TDPAC spectra of  $^{111}\text{Cd}(\leftarrow^{111}\text{In})$  embedded in 0.5 at.% In-doped ZnO.

Temperature (K)	$\omega_Q$ ( $10^6 \text{ rad s}^{-1}$ )	$\lambda_g$ ( $10^9 \text{ s}^{-1}$ )	Fraction (%)
1000	18.46(2)	0.034(14)	88(1)
873	18.37(2)	0.036(15)	87(1)
773	18.32(2)	0.025(7)	87(1)
673	18.20(2)	0.020(4)	86(1)
473	17.99(4)	0.017(4)	87(1)
298	17.87(5)	0.010(3)	87(1)

$$G_{22}^*(t) = \frac{\lambda_g}{\lambda_g + \lambda_r} + \frac{\lambda_r}{\lambda_g + \lambda_r} \exp[-(\lambda_g + \lambda_r)t], \quad (3)$$

where  $\lambda_g$  is defined as the reciprocal of the recovery time,  $\tau_g$ , to the ground state of the probe atom, and  $\lambda_r$  stands for the Abragam and Pound relaxation constant.<sup>13</sup> (At longer times, the second term of Eq. (3) becomes negligible and only the first term remains as a time-independent value. For  $\lambda_g \gg \lambda_r$ , due to very short recovery time,  $G_{22}^*(t)$  is unity and the aftereffect is not observed.) For a polycrystalline sample,  $G_{22}^{\text{static}}(t)$  in Eq. (2) is explicitly written for  $I=5/2$  as

$$G_{22}^{\text{static}}(t) = \sigma_{2,0} + \sum_{n=1}^3 \sigma_{2,n} \cos(\omega_n t). \quad (4)$$

In Eq. (4), the amplitudes  $\sigma_{2,n}$  are functions only of the asymmetry parameter  $\eta = (V_{xx} - V_{yy})/V_{zz}$  ( $0 \leq \eta \leq 1$ ) for the principal axes of the EFG chosen as  $|V_{xx}| \leq |V_{yy}| \leq |V_{zz}|$ . An EFG can be described by using the two tensor parameters,  $V_{zz}$  and  $\eta$ , for the diagonalized symmetric traceless EFG tensor. The frequencies  $\omega_n$  are related to the electric quadrupole frequency,

$$\omega_Q = -\frac{eQV_{zz}}{4I(2I-1)\hbar}, \quad (5)$$

for the asymmetry parameter  $\eta=0$  in such a way as  $\omega_1 = 6\omega_Q$ ,  $\omega_2 = 12\omega_Q$ , and  $\omega_3 = 18\omega_Q$ . In Eq. (5), the quadrupole moment of the probe nucleus at the relevant intermediate state of the cascade is  $Q=0.77(12) \text{ b}$ ,<sup>9</sup> and the other symbols have usual meanings. Because the present spectra cannot be reproduced with a single component, we assumed the presence of the second minor component forming an unknown backgroundlike plateau for all the spectra following the method applied by Asai *et al.*<sup>14</sup> The values of the parameters obtained by the least-squares fits for the 0.5 at.% In-doped ZnO are listed in Table I. The fraction of the main component giving the oscillatory structures is almost constant ( $\sim 87\%$ ) at any temperature; this result is consistent with the above interpretation that the displacement of the probe atoms is not the cause of the spectral damping. From the fits, we obtained the third observational fact that the  $\omega_Q$  values gradually increase as the temperature is raised for the 0.5 at.% In-doped sample.

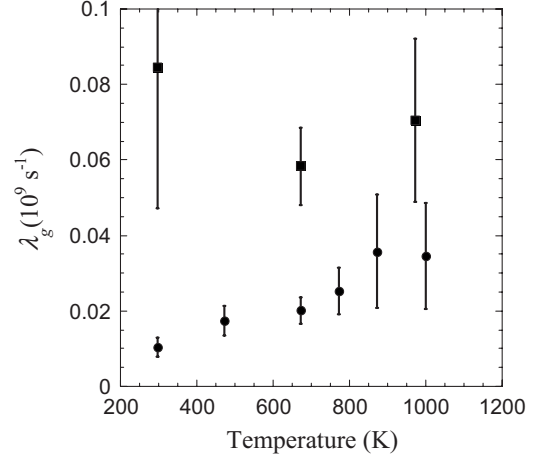


FIG. 3. Temperature dependences of the recovery constant,  $\lambda_g$ . The solid squares and circles represent the values for undoped and 0.5 at.% In-doped ZnO, respectively.

## IV. DISCUSSION

### A. Electronic behavior at the probe sites

The temperature dependence of  $\lambda_g$  was investigated in order to shed insight into the electronic state at the probe sites. The  $\lambda_g$  values obtained by the fits are plotted against the temperature in Fig. 3. For the 0.5 at.% In-doped sample, the values gradually increase as the temperature becomes higher, signifying that the probe atoms reach their ground state faster at higher temperatures. This trend is reasonably understood in the context that the probe atom returns to its ground state fast due to high refilling rate in the atomic orbital of the probe atom by abundant conduction electrons at high temperature, which explicitly reflects a property of ZnO as a donor-doped semiconductor.

In terms of the correlation between the spectral damping caused by an aftereffect and the density of conduction electrons, however, we immediately notice an inconsistent fact in our observations. In donor-doped semiconductors, the electric conductivity is, in general, enhanced as the dopant concentration is raised because of increasing conduction electrons. For ZnO doped with In as well, the conductivity enhancement has already been ascertained in bulk experiments for various dopant concentrations.<sup>15,16</sup> In such a case, the aftereffect should be less operative, as observed for another compound semiconductor  $\text{In}_2\text{O}_3$  doped with Sn, for example.<sup>17</sup> The aftereffect is indeed suppressed for  $\text{In}_2\text{O}_3$  as the concentration of a donor Sn increases: the amplitude of oscillating TDPAC spectra of the  $^{111}\text{Cd}(\leftarrow^{111}\text{In})$  probe becomes larger with increasing concentration of Sn. In the present experiment, however, it is evident from the  $\lambda_g$  values plotted in Fig. 3 that the recovery to the ground state of the probe atoms is achieved in a shorter time when they are embedded in the undoped sample; in other words, the aftereffect is more prominent in the 0.5 at.% In-doped ZnO. This behavior is completely opposite to the general understanding.<sup>7</sup> The present experimental fact evidently reveals that the probe site is not readily accessible by conduction electrons in the In-doped ZnO compared to the case of

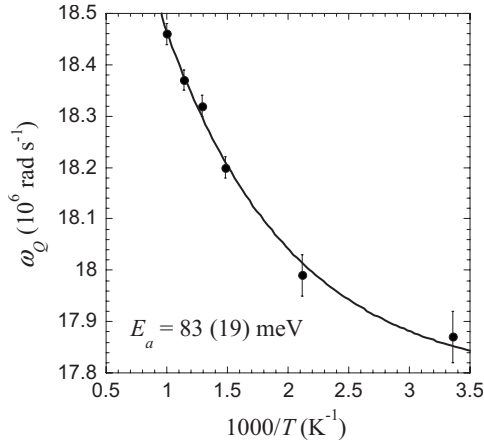


FIG. 4. Temperature dependence of the nuclear quadrupole frequency,  $\omega_Q$ , for 0.5 at.% In-doped ZnO. The data are fitted with Eq. (6).

the undoped ZnO; namely, the probe site is off the mainstream of carrier electrons when doped with an appreciable amount of In. This observation is very interesting in that the principal medium of electric conductivity is the matrix ZnO despite the fact that conductivity enhancement is realized by doping In.

The temperature dependence of the nuclear quadrupole frequency,  $\omega_Q$ , for the In-doped ZnO is also closely related to the electronic behavior at the probe site. As shown in Fig. 4, the data points are well reproduced by

$$\omega_Q(T) = \omega_Q(0) \left[ 1 + \alpha \exp\left(-\frac{E_a}{kT}\right) \right], \quad (6)$$

where  $E_a$  represents the activation energy and  $\alpha$  is a constant.<sup>15,18</sup> The activation energy was estimated to be  $E_a = 83(19)$  meV. This temperature variation is not ascribable to the thermal expansion of the lattice because the frequency increases as the temperature is raised; this may suggest that the electronic state of the probe atom changes with temperature. Since the density of electrons at the probe atom is considered to rise with increasing concentration of conduction electrons at higher temperatures, this activation energy may be associated with the donor level below the conduction-band edge.

### B. Discrete change in the extranuclear field of the probe

The unexpected behavior of the conduction electrons must be arising from a drastic change in the electronic state of the probe atom embedded in the In-doped ZnO, and it is thus considered that information on their sites could be a key to the investigation of the charge distribution surrounding the probe ions.

From the fits to the TDPAC spectra for the undoped ZnO in Fig. 2(a), the axially symmetric EFG at the  $^{111}\text{Cd}$  nucleus was estimated to be  $|V_{zz}| = 1.7(3) \times 10^{21}$  V m<sup>-2</sup> for all the temperature range,<sup>19</sup> and the fractions of the components giving this oscillating pattern were found to be almost constant: 85(1)%, 87(1)%, and 86(1)% at 973 K, 673 K, and 298 K, respectively. As reported for the identical

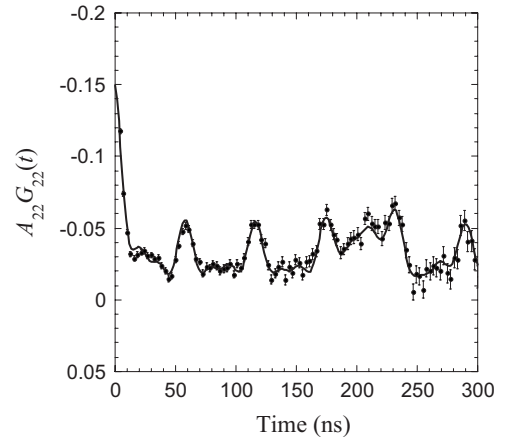


FIG. 5. TDPAC spectrum of  $^{111}\text{Cd}(\leftarrow^{111}\text{In})$  embedded in 0.05 at.% In-doped ZnO measured at 673 K. A least-squares fit was carried out assuming two different oscillating components identical to those appearing in the spectra for undoped and 0.5 at.% In-doped ZnO.

samples,<sup>15,18,20–22</sup> it is known with the help of a theoretical calculation with a point charge model that the  $^{111}\text{Cd}$  probe occupies the substitutional  $\text{Zn}^{2+}$  site.<sup>18,23</sup>

For the 0.5 at.% In-doped ZnO, on the other hand, the magnitude of the EFG deduced from the  $\omega_Q$  value listed in Table I is  $|V_{zz}| = 6.1(9) \times 10^{21}$  V m<sup>-2</sup> [ $\eta = 0.10(3)$ ] at room temperature.<sup>19</sup> As shown in Table I, the fraction of the main component does not fluctuate at different temperatures for this sample either; moreover, it takes almost the same value as that for the undoped sample. These observations suggest that the probe ions in the 0.5 at.% In-doped ZnO also substitute for the lattice  $\text{Zn}^{2+}$  sites. However, it is obvious that there is a significant difference in the EFG value between the undoped and 0.5 at.% In-doped samples despite the same residential site assumed, which signifies that the charge distribution surrounding the probe drastically changes between the samples. As shown in Fig. 5, we have an experimental evidence that two different oscillating components identical to those appearing in the spectra for the 0.5 at.% In-doped and undoped ZnO coexist at the total fraction of  $\sim 86\%$  for more dilute (0.05 at.%) In-doped ZnO prepared by the same method. This fact indicates that the EFG, or more specifically, the surroundings of the probe discretely but not gradually change, which cannot be explained by progressive structural deformation such as lattice distortion with increasing In impurities. It can be inferred as a possibility that a certain type of local association of In ions is formed with their increasing concentration.<sup>16</sup> For unequivocal determination of the probe site in the 0.5 at.% In-doped ZnO sample, a reliable theoretical calculation such as the density-functional theory needs to be applied.

### V. SUMMARY AND CONCLUSIONS

In this work, we measured the local fields at the  $^{111}\text{Cd}(\leftarrow^{111}\text{In})$  probe introduced in 0.5 at.% In-doped and undoped ZnO compounds by means of the TDPAC technique. We have obtained the following information on modification of

the local structure in the vicinity of the probe caused by the doping of a macroscopic amount of In. (i) For the 0.5 at.% In-doped sample, the aftereffect arising from the orbital electron capture decay of  $^{111}\text{In}$  was observed through the damping trend of the spectral amplitudes at lower temperatures. The temperature dependence clearly displays a property of the In-doped ZnO as a semiconductor: the refilling of the holes in the outermost shell of the atomic orbital with conduction electrons speeds up at higher temperatures. On the other hand, however, an unexpected local behavior of conduction electrons has been disclosed: they avoid getting access to the probe atom in spite of enhanced electric conductivity by In-donor doping. This intriguing observation is attributed to the change in local electronic structure produced by macroscopic doping of In. (ii) A gradual increase of the nuclear quadrupole frequency with rising temperature for the 0.5 at.% In-doped ZnO was observed. We consider that the relevant activation energy,  $E_a=83(19)$  meV, is associated with the donor level of In dopants below the conduction-band edge. (iii) Most of the doped In occupy the substitutional  $\text{Zn}^{2+}$  sites for both of the samples although there is a large difference of more than three times in the magnitude of the EFG between the two samples. It was found in addition

that the change in the field is not gradual but discrete, which excludes the possibility of a progressive lattice distortion for the origin of the distinct fields.

In the TDPAC spectroscopy, the aftereffect has been regarded as interference in the measurement of local fields due to analytical ambiguity arising from spectral damping. However, the present work successfully suggests that local electronic structures in the vicinity of impurities can be probed through this effect on the contrary. For further information on the behavior of conduction electrons and the probe site in In-doped ZnO, dopant concentration dependence is now under investigation.

#### ACKNOWLEDGMENTS

We thank S. Kawata for helpful instructions in the sample evaluation. Enlightening discussions on the probe sites with H. Akai and Y. Yamada are gratefully acknowledged. We express our gratitude to T. Saito and Y. Yamaguchi for providing experimental apparatus for the TDPAC measurements. The present work was accomplished in part under the Visiting Researcher's Program of the Kyoto University Research Reactor Institute (KURRI).

- 
- <sup>1</sup>S. F. J. Cox, E. A. Davis, S. P. Cottrell, P. J. C. King, J. S. Lord, J. M. Gil, H. V. Alberto, R. C. Vilão, J. Pirotto Duarte, N. Ayres de Campos, A. Weidinger, R. L. Lichti, and S. J. C. Irvine, *Phys. Rev. Lett.* **86**, 2601 (2001).
- <sup>2</sup>K. Shimomura, K. Nishiyama, and R. Kadono, *Phys. Rev. Lett.* **89**, 255505 (2002).
- <sup>3</sup>B. K. Meyer, H. Alves, D. M. Hofmann, W. Kriegseis, D. Forster, F. Bertram, J. Christen, A. Hoffmann, M. Straßburg, M. Dworzak, U. Habocek, and A. V. Rodina, *Phys. Status Solidi B* **241**, 231 (2004).
- <sup>4</sup>J. Han, P. Q. Mantas, and A. M. R. Senos, *J. Eur. Ceram. Soc.* **21**, 1883 (2001).
- <sup>5</sup>V. Bhosle, A. Tiwari, and J. Narayan, *J. Appl. Phys.* **100**, 033713 (2006).
- <sup>6</sup>S. Müller, D. Stichtenoth, M. Uhrmacher, H. Hofsäss, C. Ronning, and J. Röder, *Appl. Phys. Lett.* **90**, 012107 (2007).
- <sup>7</sup>H. Frauenfelder and R. M. Steffen, in  *$\alpha$ -,  $\beta$ -, and  $\gamma$ -Ray Spectroscopy*, edited by K. Siegbahn (North-Holland, Amsterdam, 1965), Vol. 2, p. 997.
- <sup>8</sup>G. Schatz and A. Weidinger, *Nuclear Condensed Matter Physics* (Wiley, New York, 1996).
- <sup>9</sup>R. B. Firestone, in *Table of Isotopes*, 8th ed., edited by V. S. Shirley (Wiley, New York, 1996), Vol. 1.
- <sup>10</sup>A. G. Bibiloni, J. Desimoni, C. P. Massolo, L. Mendoza-Zelis, A. F. Pasquevich, F. H. Sanchez, and A. Lopez-Garcia, *Phys. Rev. B* **29**, 1109 (1984).
- <sup>11</sup>A. G. Bibiloni, C. P. Massolo, J. Desimoni, L. A. Mendoza-Zelis, F. H. Sanchez, A. F. Pasquevich, L. Damonte, and A. R. Lopez-Garcia, *Phys. Rev. B* **32**, 2393 (1985).
- <sup>12</sup>U. Bäverstam, R. Othaz, N. de Sousa, and B. Ringström, *Nucl. Phys. A* **186**, 500 (1972).
- <sup>13</sup>A. Abragam and R. V. Pound, *Phys. Rev.* **92**, 943 (1953).
- <sup>14</sup>K. Asai, F. Ambe, S. Ambe, T. Okada, and H. Sekizawa, *Phys. Rev. B* **41**, 6124 (1990).
- <sup>15</sup>R. Wang, A. W. Sleight, R. Platzer, and J. A. Gardner, *J. Solid State Chem.* **122**, 166 (1996).
- <sup>16</sup>T. Moriga, D. D. Edwards, T. O. Mason, G. B. Palmer, K. R. Poepplmeier, J. L. Schindler, C. R. Kannewurf, and I. Nakabayashi, *J. Am. Ceram. Soc.* **81**, 1310 (1998).
- <sup>17</sup>S. Habenicht, D. Lupascu, M. Uhrmacher, L. Ziegeler, K.-P. Lieb, and ISOLDE Collaboration, *Z. Phys. B: Condens. Matter* **101**, 187 (1996).
- <sup>18</sup>H. Wolf, S. Deubler, D. Forkel, H. Foettinger, M. Iwatschenko-Borho, F. Meyer, M. Renn, W. Witthuhn, and R. Helbig, *Mater. Sci. Forum* **10-12**, 863 (1986).
- <sup>19</sup>The large uncertainty of the EFG is due to the propagation of the error of the  $Q$  moment.
- <sup>20</sup>Th. Agne, Z. Guan, X. M. Li, H. Wolf, and Th. Wichert, *Phys. Status Solidi B* **229**, 819 (2002).
- <sup>21</sup>Th. Agne, Z. Guan, X. M. Li, H. Wolf, Th. Wichert, H. Natter, and R. Hempelmann, *Phys. Lett.* **83**, 1204 (2003).
- <sup>22</sup>T. Agne, M. Diecher, V. Koteski, H.-E. Mahnke, H. Wolf, and Th. Wichert, *Hyperfine Interact.* **159**, 55 (2005).
- <sup>23</sup>S. Deubler, J. Meier, R. Schütz, and W. Witthuhn, *Nucl. Instrum. Methods Phys. Res. B* **63**, 223 (1992).